ELSEVIER

Journal of Structural Geology 27 (2005) 1925–1939

JOURNAL OF STRUCTURAL GEOLOGY

www.elsevier.com/locate/jsg

Tectonic geomorphology of the Red Rock fault, insights into segmentation and landscape evolution of a developing range front normal fault

Nathan W. Harkins[1], David J. Anastasio*, Frank J. Pazzaglia

Department of Earth and Environmental Sciences, Lehigh University, 31 Williams Drive, Bethlehem, PA 18015, USA

Received 10 January 2005; received in revised form 13 June 2005; accepted 13 July 2005
Available online 13 September 2005

Abstract

The Red Rock fault, an active normal fault in southwest Montana, is reevaluated for fault segmentation using a multiproxy approach. Field characterization of soils coupled with radiocarbon ages in offset hanging wall fans and terraces constrain the rupture history at a number of locations along strike. These data are coupled with morphometric analysis of dated alluvial fan deposits and adjacent 2nd and 3rd order footwall drainage basins to further constrain fault kinematics and segmentation. Morphometric analysis of the Big Sheep Creek catchment, which drains a large area of the footwall range, provides a control on the spatial extent of fault influence on footwall topography. Three fault segments are recognized by this study, compared with the two segments recognized previously. Data from offset alluvial surfaces were synthesized with hanging wall fan and footwall drainage basin data to demonstrate a southward increase in displacement along the Red Rock fault since at least the latest Pleistocene, at a maximum rate of 1.5 mm/yr. Red Rock ruptures were mainly confined to segments, suggesting a fault behaving as several discrete slip surfaces; however, simultaneous rupture of adjacent segments during one event indicates some fault zone coalescence. A youthful Red Rock fault is supported by the absence of tectonic influences on footwall topography and is consistent with an eastward progression of normal fault development along the northern arm of the Yellowstone hot spot.

Keywords: Neotectonics; Segmentation; Geomorphology; Northern Rocky Mountains; Landscape evolution

1. Introduction

Active fault zones can be complex features with multiple, discrete slip surfaces that communicate strain broadly. Geometric and kinematic complexity is manifested by the distinct segments observed along many map scale fault zones and is especially prominent along active range front normal faults. A fault segment may possess and be delineated by a unique set of one or more physical properties such as characteristic seismicity, rupture frequency and spatial extent, strike orientation, scarp morphology, footwall topography, and hanging wall fan geometry (Dodge and Grose, 1980; Schwartz et al., 1982; DePolo et al., 1991; Turko and Knuepfer, 1991; Wheeler, 1987; McCalpin, 1996). Establishing a valid model for segment development and evolution holds important implications for the subsurface geometry of a fault system and its seismogenic properties. One model holds that segments are inherited from the geometry of a fault system in the early stages of its development. In this paradigm, segments are initiated as isolated slip surfaces that evolve due to linkage into multi-segment fault zones, where fault strands interact and eventually smooth (Cowie, 1998). Comparing fault segments in various stages of development provides empirical tests of this model.

In this study, we use a variety of geomorphologic data to refine segmentation characterization along the Red Rock fault, a range front normal fault in southwestern Montana that exhibits prominent Quaternary fault scarps and significant along strike morphologic variation (Fig. 1). Previously, two segments were identified along the Red Rock fault but disagreement exists as to the location of the segment boundary (Haller, 1988; Greenwell, 1997). By utilizing a diverse suite of data, collected from the footwall, hanging wall, and along fault scarps, we resolve the locations of segment boundaries, characterize the recent

* Corresponding author. Tel.: +1 610 758 5117; fax: +1 610 758 3677.
E-mail addresses: nharkins@geosc.psu.edu (N.W. Harkins), dja2@lehigh.edu (D.J. Anastasio), fjp3@lehigh.edu (F.J. Pazzaglia).
[1] Present address: Department of Geosciences, Pennsylvania State University, Deike Building, University Park, PA 16802, USA.

0191-8141/$ - see front matter © 2005 Elsevier Ltd. All rights reserved.
doi:10.1016/j.jsg.2005.07.005

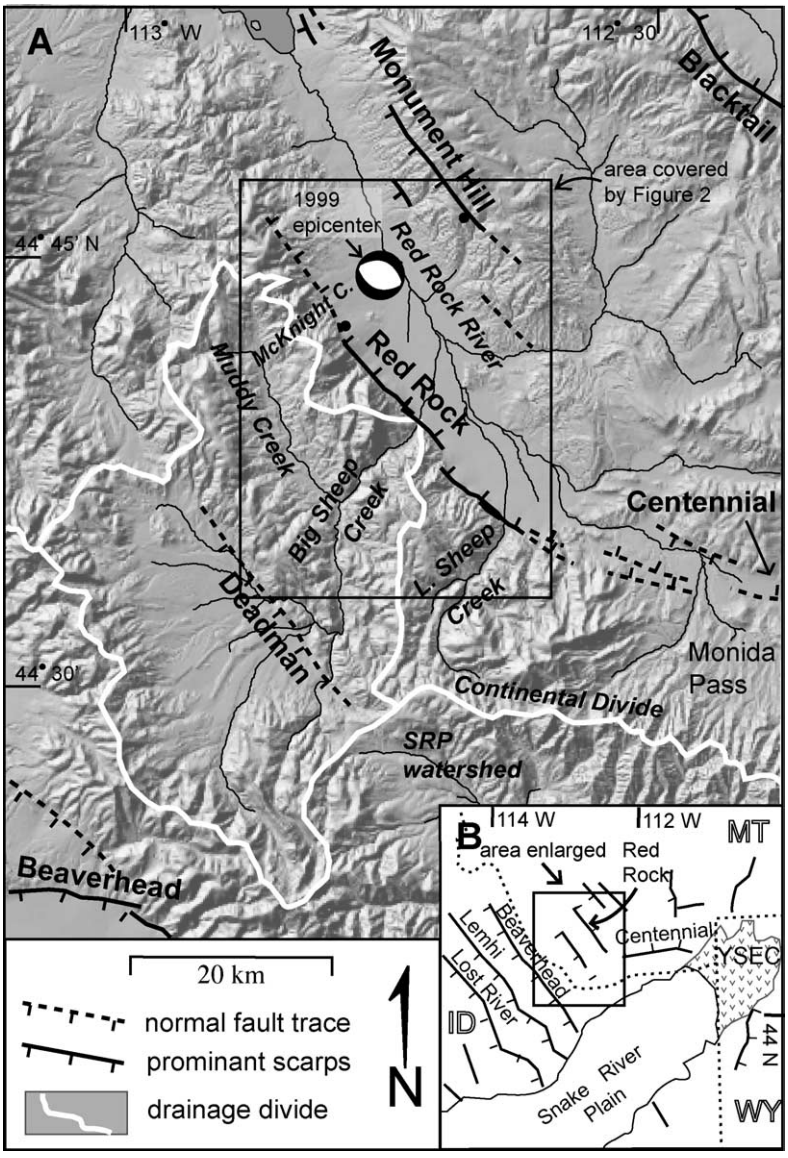

Fig. 1. (A) Regional setting of the Red Rock fault. Inset map (B) displays the location of the Red Rock fault in relation to the Snake River Plain, Yellowstone eruptive center (YSEC), and other active faults associated with the Centennial Tectonic belt. On the hillshade map; the Red Rock and other nearby active normal faults are shown, including the Monument Hill and western tip of the Centennial fault system. Big Sheep Creek is the largest catchment in the Red Rock footwall, with its southern boundary forming the continental divide between the greater Missouri and Snake River Plain (SRP) watersheds. The fault plane solution and approximate epicenter of the 1999 5.3 m_b Red Rock Valley is shown (Stickney and Lageson, 2002).

slip behavior on the various segments, and draw conclusions about the long-term history of the Red Rock fault.

Recent motion along the fault was determined from offset alluvial fan and terrace deposits that were dated by ^{14}C. Segmentation along the Red Rock fault as defined by landforms offset by recent fault ruptures provide a spatial and temporal framework in which to examine other records of segmentation preserved in the landscape. These records include the mapped distribution of dated alluvial fan units, which preserve a record of the relative magnitude and distribution of accommodation space in the down-dropped hanging wall (Bull, 1961; Denny, 1967), and a series of channel and drainage basin metrics extracted from footwall catchments, which record fluvial response to offset at the range front. Individual rupture events can be resolved from offset landforms. In contrast, hanging wall fan and footwall drainage basin metrics respond to fault-related tilting and base level changes that integrate longer-term histories of fault activity. Together, these multiproxy reconstructions of fault activity add credence to slip rate determinations. Comparison of these data provides insight into the temporal resolution of common metrics used to define segments, and resolves segmentation evolution of the Red Rock fault.

2. Geologic setting

The NW–SE-trending Red Rock fault is an east dipping

normal fault along the eastern side of the Tendoy Mountains, in southwestern Montana (Fig. 1). Regionally, the Red Rock fault is one of many active normal faults associated with the Centennial Tectonic Belt, an arm of the Intermountain Seismic Belt stretching westward from the Yellowstone region along the northern flank of the Snake River Plain. Red Rock Valley is being extended between the Red Rock fault on the west, the north dipping Centennial fault to the southeast and the west dipping Monument Hill fault to the northeast. Farther to the west are the Beaverhead, Lemhi, and Lost River Ranges, each of which are cored by Paleozoic or older metasedimentary rocks and bound on their western flanks by an active range front normal fault. The close proximity of faults within the Centennial Tectonic Belt to the Snake River Plain has led several authors to infer a causal relationship between passage of the Yellowstone hot spot between 6.5 and 4 Ma and Red Rock fault inception (Anders et al., 1989; Pierce and Morgan, 1992; Anders; 1997; Densmore et al., 2004).

Along the eastern Tendoy Range, the Red Rock fault outcrops as scarps in bedrock and alluvium beginning just

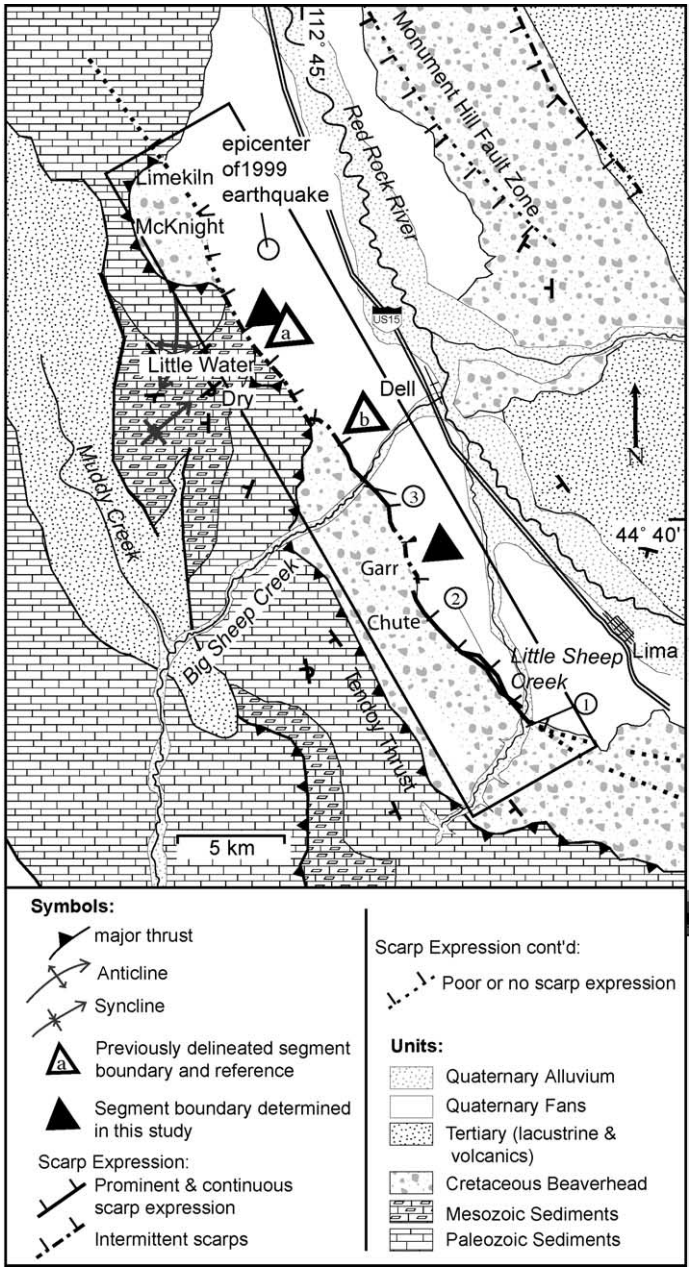

Fig. 2. Geologic map of the Red Rock fault. Names of some of the proximal footwall drainage basins are shown for spatial reference. The triangle marked 'a' shows the segment boundary defined by Haller (1988) on the basis of scarp morphology, while that marked 'b' shows the boundary marked by Greenwell (1997) on the basis of fan metrics. Locations of the trenching study (**1**) (Stickney et al., 1987), multiple scarps (**2**), and the knick point in Big Sheep Creek (**3**) are marked. Boxed area is detailed in Fig. 3.

south of Little Sheep Creek and continuing northward discontinuously to near McKnight Canyon (Fig. 2). From Little Sheep Creek to Chute Canyon, the fault shows dramatic topographic expression, with multiple scarps and prominent footwall faceted spurs that rise abruptly above Red Rock Valley. North of McKnight Canyon, the fault trace lacks faceted spurs or obvious scarps in late Quaternary units, but is evident on aerial photos until just north of Limekiln Canyon. The total strike length of the Red Rock fault is ~34 km. An intermittent, more E–W striking suite of fault traces were identified south of Little Sheep Creek, in the vicinity of Monida Pass (Fig. 1). These features may be related to the nearby, similarly striking Centennial fault system. Distribution of strain throughout the Red Rock valley is complex. The northern Red Rock fault and the southern extent of the Monument Hill fault system likely communicate NE–SW oriented extensional strain across the Red Rock valley given the close proximity, parallel strike, and coseismic behavior (the 1999 5.3 m_b 'Kidd Earthquake'; Stickney and Lageson, 2002).

The Red Rock fault offsets variable lithologies and Sevier thrust related structures within the footwall Tendoy range (Fig. 2) (Scholten et al., 1955; Klecker, 1980; Lonn et al., 2000; Harkins et al., 2002, 2003). In the southern and central portions of the footwall, from Little Sheep Creek to Big Sheep Creek, the fault offsets extensive deposits of synorogenic conglomerates of the Late Cretaceous Beaverhead Group (Williams, 1984; McDowell, 1989). Farther hinterland (west), Sevier thrust sheets comprised of Paleozoic carbonate and clastic units underlie the higher peaks of the Tendoy Mountains. A small salient in the front of the Tendoy thrust sheet in the vicinity of Little Water Canyon results in the Red Rock fault locally offsetting Paleozoic and lower Mesozoic units. Here, structural thickening above a ramp corner produced a kilometer-scale anticline–syncline pair at the range front. Farther north, where the Tendoy thrust arcs back to the west, the Red Rock fault again offsets Beaverhead Group strata. The fault eventually dies out in Mississippian units at its northern terminus.

A sharp topographic contrast exists between the hanging wall and footwall of the Red Rock fault. The hanging wall is capped with fan gravels that are generated in the Tendoy Mountains and slope gently eastward from the range towards the Red Rock River. Farther east, bedding within extrusive and sedimentary units of the hanging wall (Neogene Sixmile Creek Formation and the Timber Hill basalt) slope gently to the southwest (Fields et al., 1985). In the footwall of the Red Rock Fault, the Tendoy Mountains rise above the Red Rock valley with a maximum relief of 1.1 km (at Dixon Mountain). The 8–12-km-wide range is deeply incised by the transverse canyons of Big and Little Sheep Creeks. Big Sheep Creek possesses a particularly large catchment, extending westward to the crest of the Beaverhead Range (Fig. 1). The footwall between the transverse streams is incised by a number of small drainage basins with ephemeral streams.

Multiple allostratigraphic alluvial fan units are identified on the Red Rock hanging wall. The fan units possess distinct sedimentology and morphology. Fans are found at many locations along strike, are correlative between locations, and are offset by faulting. Fault scarps also offset river terraces that are genetically related to the fan deposits in both Little and Big Sheep Creeks. A 4 m scarp in the alluvial surfaces at Big Sheep Creek is accompanied by a knick-zone in the channel ~25 m upstream from the fault trace. A 3 m scarp at Little Sheep Creek is adjacent to a set of uplifted terraces in the proximal footwall (Johnson, 1981; Haller, 1988).

2.1. Previous Red Rock fault studies

Trenching, fault scarp morphology, fan metrics, and limited topographic analysis have been completed to qualitatively and quantitatively describe the segmentation behavior of the Red Rock fault. A trench dug across the fault scarp at the mouth of Little Sheep Creek yielded evidence of two offsets over the last 10–15 kyrs (Stickney et al., 1987) (Fig. 2). The younger offset was dated at 3000 ± 800 years and a minimum age on the older offset was estimated to be ~9 kyr.

Based on scarp morphologies, two segments were proposed along the Red Rock fault. These segments have been coined the Sheep Creeks segment in the south and the Tiber Butte segment in the north, with a segment break just north of Big Sheep Creek (Johnson, 1981; Haller, 1988; Crone and Haller, 1991) (Fig. 2). A few locations south of Garr Canyon exhibit multiple scarp traces, which Crone and Haller (1991) interpret as at least two discrete offset events separated by 5–7 kyrs. North of the proposed segment break, scarps are generally shorter, less steep, and discontinuous.

Greenwell (1997) used variation in fan morphology between the northern and southern Red Rock hanging wall to relocate northward the Sheep Creeks and Timber Butte segment break to near Little Water Canyon. Small steep fans in the south were interpreted to record greater accommodation space afforded by greater fault offset and broad gentle fans in the north as an indication of less accommodation space due to less fault offset of the northern segment (Greenwell, 1997). Utilizing footwall catchment size, relief, and slope, Densmore et al. (2004) highlight morphological differences between the northern basins and those south of Big Sheep Creek. The analyses provide evidence of northward diminishing displacement along the Red Rock fault, but do not resolve the placement of segment boundaries. In this study, we use diverse data to characterize segmentation and rupture patterns along the Red Rock fault since the Pleistocene.

3. Methods

Proximal hanging wall fans, footwall fan heads, and visible fault scarps were mapped from 1:30,000 scale vertical aerial photos and field mapping at 1:24,000 scale. Additionally, footwall terraces along Big Sheep Creek were mapped and surveyed along the river valley (Fig. 2). Multiple alluvial fan units and terrace levels, like those exposed in the Red Rock Valley, primarily result from climatic change rather than tectonically driven local base level fall (Lustig, 1965; Ritter et al., 1993). Four fan units (Qft1 through Qft4) were mapped on the basis of sedimentology, stratigraphy, fan surficial morphology, and a field-based soil chronosequence. Soil pits dug into proximal footwall fan surfaces at the mouths of drainages provided material for both absolute and relative dating of fans. Soil profiles were described down to a depth of at least 1 m and detrital charcoal was collected for ^{14}C analysis. In the absence of datable material, relative development of pedogenic carbonate was used for age constraint and to correlate fan deposits along the range front. Terraces along Big Sheep Creek were subjected to a similar suite of analyses in order to better constrain a local soil development chronosequence, to establish a temporal link between hanging wall fan and footwall terrace generation, and to evaluate the effects of Red Rock fault activity on an antecedent fluvial system. A temporal link established between fault proximal fan units and terraces observed elsewhere in the landscape validates the assumption that fan deposition was largely climatically modulated.

Soils in semi-arid climates, like that in the American west, accumulate pedogenic carbonate over time. We used a three-class system in the field to characterize the degree of carbonate soil development, from Class I (poorly developed) to Class III (very well developed). Pedogenic carbonate generally increases with the age of a soil, but is also strongly influenced by other factors including parent material, aerosolic dust content, and local root respiration rates (Gile et al., 1966; Birkeland, 1999). Clast counts were conducted at pit sites to determine the relative percentage of carbonate in the parent material. A number of previous studies calibrated carbonate stage development to absolute soil ages determined from ^{14}C analysis of detrital charcoal (Reheis, 1987; Ritter et al., 1993). We used variations in pedogenic carbonate in 10 soil pits and five new ^{14}C dates to correlate fan and terrace deposits (Table 2) in the hanging wall and footwall of the Red Rock fault.

The ages of various fan units offset by the fault provide boundary ages for the most recent surface rupture. Map patterns of hanging wall fan units are also a crude measure of recent tectonism. Channelized fan units indicate entrenchment of older materials and imply a lack of sediment accommodation space in the hanging wall. Comparatively, broad, lobate exposures indicate blanketing deposition of younger fan units over older materials implying an ongoing generation of accommodation space.

Topographic analyses of the footwall ranges were conducted to identify the manifestation of faulting on footwall fluvial systems. The geometries of 21 ephemeral drainage basins emptying eastward into the Red Rock Valley along with Big Sheep Creek were quantitatively described using slope long profiles, length gradient indices, basin hypsometries, volume/area ratios, basin shapes, and slope asymmetries (Table 1). With the exception of Big Sheep Creek, these analyses were limited to drainage basins of similar areas (1–5 km^2) and orders (2–3), contained within watersheds mainly underlain by the Beaverhead Group. Additionally, several basins not hydrologically connected to the fault but also underlain by the Beaverhead Group were analyzed for controls. The control basins are located at the southern end of Red Rock valley, south of the southern terminus of the Red Rock fault. Digital elevation models (DEMs), (30 m resolution available from the USGS) were used to characterize topography and to evaluate

Table 1
Footwall drainage basin geomorphic indices utilized in this study. Sensitivity refers to the specific basin property sampled by each metric

Metric	Symbol	Equation	Variables	Senstivity
Stream length gradient index[a]	SL	$SL = (\Delta H/\Delta L)L$	L; distance from channel mouth ΔH; interval channel elevation change ΔL; interval channel distance	Channel slope
Hypsometric integral[b]	V/HA	$V/HA = \int x\,dy$	$x\,dy$; basin area x over elevation interval dy	Basin area–altitude distribution (3-D basin shape)
Basin volume/area[c]	V/A	$V/A = V_i/A_i$	V_i; basin volume A_i; basin planemetric area	Normalized basin volume (3-D basin shape)
Basin asymmetry[d]	AF	$AF = 100(A_r/A_t)$	A_r; area of one basin side A_t; total basin area	Basin area distribution (2-D basin shape)
Basin elongation[e]	E_r	$E_r = D_l/D_s$	D_l; basin long axis length D_s; basin short axis length	Basin geometry (2-D basin shape)

[a] Hack (1973).
[b] Strahler (1952) and Pike and Wilson (1971).
[c] Frankel (2002).
[d] Hare and Gardner (1985) and Cox (1994).
[e] Bull and McFadden (1977).

Table 2
Age controls derived from soil profiles, pedogenic carbonate development, and radiocarbon analysis for the five fluvial terrace and alluvial fan surface generations recognized along Big Sheep Creek and in the Red Rock fault hanging wall fans

Terrace and alluvial fan unit age controls							
Site #	Location	Horizon	Depth (cm)	Carbonate stage	^{14}C age[a]	Alluvial terrace unit	Age range
1	Garr Canyon[b]	A	0–22	I	N/A	Oft4	Late Holocene (<3 ka)
		Bk	22–70				
		Bkb	70–106	II (buried soil)			
		C	106–113				
2	Big Sheep Creek (*D*)	A	0–16	I	1290±40		
		Bk	16–52				
		C	52–200+				
3	Little Water Canyon[b]	A	0–25	I	N/A		
		Bk	25–63				
		Cb	63–75				
		C	75–100				
4	Big Sheep Creek (*U*)			I	N/A		
5	Chute Canyon[b]	Ac	0–24	I+ to II	4560±60	Qft4a	Middle Holocene (5–3 ka)
		Bt	24–40		(bulk)		
		Bk	40–65				
		Btk	65–105				
		C	105+				
6	Dry Canyon[b]	A	0–16	I+ to II			
		Bk	16–77		3230±40		
		CbK	77–111		3520±40		
		C	111–120				
7	Big Sheep Creek (*D*)	Bk	0–59	II+	10480±60		
		Ck	60–110				
8	Big Sheep Creek (*D*)	A	0–25	II+ to III−	N/A	Qft3	Latest Pleistocene (~20–10 ka)
		Btk	25–41				
		Bk	41–90				
		Ck	90+				
9	Dry Canyon[b]	A	0–13	III	N/A		
		Bk	13–62				
		Bc	62–80				
		Cb	80–110				
10	Mouth of Muddy Creek (*U*)			II+ to III−	N/A		
						Qft2	Late Pleistocene (Bull Lake, stage 6?)
						Qft1	Middle Pleistocene (?)

U Soil pit located upstream of Quadrant. *D* Soil pit located downstream of Quadrant Fm. exposures.
No soil pits in Qft2 or Qft1 surfaces
Qft2 age estimate based on projection of surfaces to glacial deposits in the headwaters
Qft1 age unknown, but likely significantly older than Qft2 based on elevation above other terrace surfaces
[a] Calibrated (calendric) radiocarbon ages are displayed in years B.P. with 2σ ranges.
[b] Soil pit located in the Red Rock Valley.

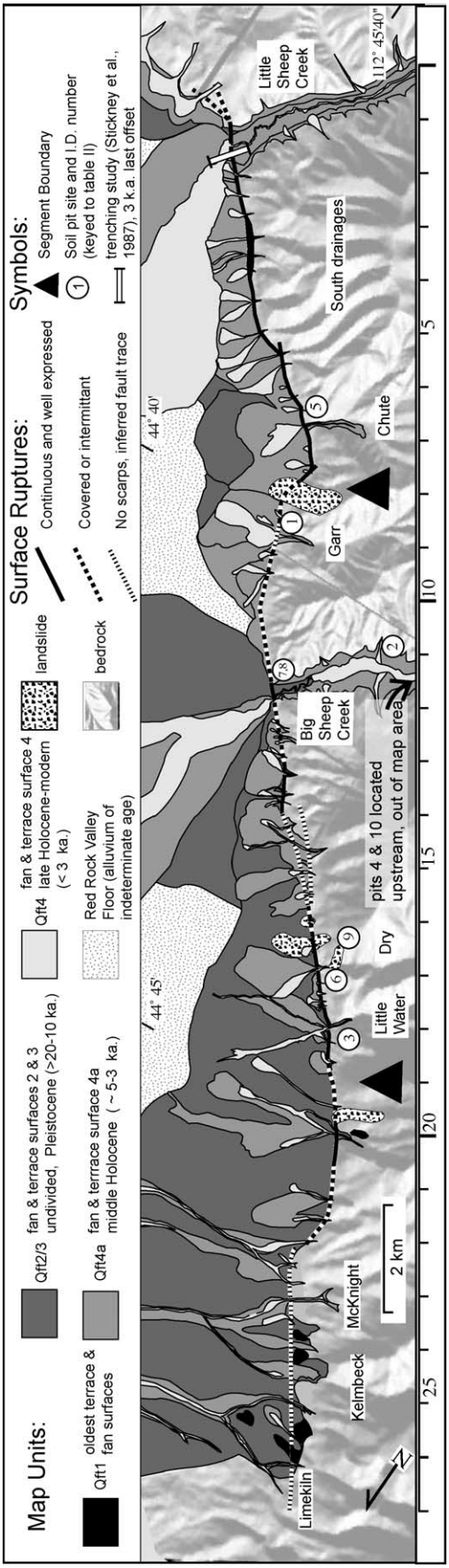

Fig. 3. Map of scarps, Quaternary fan and terrace units identified along the Red Rock fault. Locations of age control, the trenching study of Stickney et al. (1987), and major named drainages are shown. Segment boundaries delineated by this study are based on the relationship of these fan and terrace units to fault ruptures. Numbers along the bottom of the figure are used for spatial reference in the text and are equal to kilometers along strike north of the approximate southern fault terminus.

landscape evolution (Franklin, 1987). Channel profiles were extracted from the DEMs starting at the mapped fault trace and extending upstream. The profiles were smoothed over a 3–5 point data window and normalized to elevations at the fault trace for visual, qualitative comparison. Length–gradient (*SL*) indices normalize channel slope to basin size, providing a means to quantitatively compare channel slope between basins (Table 1). Length gradient indices were calculated using a 300 m tapered aperture window in order to resolve small (<0.5 km) deviations in channel slope.

Basin hypsometry and volume–area (*V/A*) ratios describe the three-dimensional shape of a basin and reflect the relative degree of channel incision over an entire watershed. Basin hypsometry quantifies the elevation distribution of surface area in a watershed. Hypsometric curves are calculated based on total basin area and total relief within a catchment and are thus normalized and comparable between basins. Hypsometric integrals quantify basin area–elevation distribution, small values are indicative of large basin areas at lower elevations and large values indicate a predominance of basin area at higher elevations. *V/A* ratios reflect the average depth of a basin relative to basin surface area. *V/A* ratios are derived from topographic data sets by comparing calculated basin volume beneath an upper enveloping surface (pinned to the drainage divides) and basin planimetric area.

Drainage basin elongation and asymmetry describe only the planimetric shape of a watershed and are insensitive to vertical basin geometry. Elongation is quantified by comparing basin major and minor axes, measured through a geometric midpoint. Asymmetry is measured by comparing the area distributed on either side of a trunk channel and may reflect regional tilting orthogonal to channel orientation. Terrace elevations and footwall channel slopes were surveyed along Big Sheep Creek and extracted from DEMs for ~20 km upstream of the fault. Terrace strath and fill top elevations were measured to 1 m accuracy relative to the modern channel with an altimeter and a measuring tape.

4. Results

4.1. Fan and terrace stratigraphy

Ten soil pits were dug into fan and terrace surfaces; four yielded charcoal suitable for analysis (Table 2, Fig. 3). Four fan ages are defined along the Tendoy Range front, ranging in age from late Holocene to Pleistocene. The alluvial deposits were identified and correlated along strike on the basis of surface morphology and soil development.

4.1.1. Qft1

Qft1 is the oldest surficial unit in the field area. Exposures of Qft1 are limited to a few isolated deposits at the northern end of the Red Rock fault, near Limekiln and

Kelmbeck canyons (Fig. 3, km 24–26) and on rare, intermittent, high gravel capped surfaces along Big Sheep Creek. In the Red Rock Valley, Qft1 exposures are composed of rounded to sub-angular gravel, sand, and silt. Clasts are predominantly limestone with lesser amounts of rounded quartzite, exhibiting affinities to the Paleozoic and Cretaceous bedrock exposed in the Tendoy Mountains. Along Big Sheep Creek, Qft1 gravels cap Paleozoic bedrock straths and are rich in quartzite cobbles and boulders derived from Precambrian quartzites exposed in the headwaters of the Big Sheep Creek drainage. Deposits of Qft1 fans are incised by stream channels filled with younger units (Fig. 3). Along Big Sheep Creek, Qft1 treads exhibit a very smooth surface morphology and are 5–10 m higher than the next younger, inset alluvial surface. No charcoal was recovered from Qft1 deposits; however, landscape position above dated late Pleistocene deposits, thick (3–5 mm) carbonate rinds on cobbles, and smooth fan surface morphology suggest a middle Pleistocene age.

4.1.2. Qft2

Qft2 surfaces are positively identified only along Big Sheep Creek. Qft2 terraces are bedrock straths 8–15 m above modern channel elevations, capped by 0.5–2 m of gravel fill. The terrace gravels are rich in well-rounded quartzite cobbles and carbonate clasts derived from Sevier thrust sheets. Qft2 surfaces are distinguished at elevations between recognized Qft1 and Qft3 surfaces. Qft2 surfaces project into late Pleistocene glacial moraines in the headwaters of Big Sheep Creek. Where definitive, Qft2 fan surfaces are similar in surface morphology to Qft3 fan surfaces. This required mapping Qft2/3 as undivided in the Red Rock valley (Fig. 3).

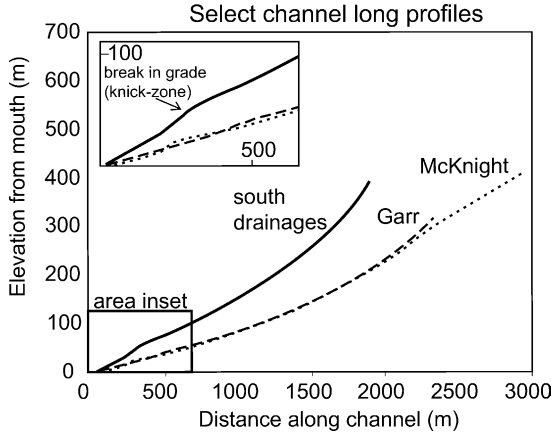

Fig. 4. Selected channel long profiles extracted from footwall drainage basins distributed along strike. Channel elevations are normalized to the channel mouth altitude. The south drainages profile (solid line) is representative of profiles extracted from Little Sheep Creek to just south of Chute Canyon. Locations of the other long profiles are identified on Fig. 5. A significant break in grade and channel convexity is observed in the lower 0.5 km of the southern drainages.

4.1.3. Qft3

Qft3 and Qft2/3 deposits blanket the Red Rock hanging wall north of Big Sheep Creek with fewer exposures south of the creek. The exposures fine and coalesce down fan with a very smooth or subdued bar and swale surface morphology. Along the northern Red Rock piedmont, valleys filled with younger fan units are inset into Qft2/3 fan surfaces. Fan gravels are composed of materials derived locally from the immediate footwall. Along Big Sheep Creek, the Qft3 surfaces are bedrock straths ~3–8 m above the modern channel and are capped with one to several meters of gravel fill. Qft3 gravel composition is similar to Qft2, but with lesser amounts of quartzite. Qft3 soil pits exhibit well-developed, stage II+ to III pedogenic carbonate horizons and buried soil horizons. A radiocarbon age of ~10.5 kyr from charcoal from near the top of a Qft3 soil pit at Big Sheep Creek can be regarded as a minimum age for this unit. Soil profiles, fan surface morphology, and the widespread distribution of Qft3 are similar to the Qf3 deposits of the Cedar Creek alluvial fan described by Ritter et al. (1993). A late Pleistocene to latest Pleistocene age (~20–10 kyr) is proposed for its deposition.

4.1.4. Qft4a

Surface exposures of Qft4a are broad and extensive adjacent to the southern Red Rock fault (Fig. 3, km 0–10) but are confined to inset valleys farther north (Figs. 3 and 4). Qft4a exhibits a subdued but clearly identifiable bar and swale surface morphology. Clast composition is similar to the older Qft3 unit. Qft4a terraces along Big Sheep Creek are extensive, broad bedrock straths capped with 0.5–2 m of gravel that lie 1–3 m above the modern river. Qft4a soil pits exhibit stage I+ to II pedogenic carbonate development. Charcoal from near the top of Qft4a deposits from two soil pit sites yielded radiocarbon ages of 4.6–3.2 kyr (Table 2). Qft4a deposition is regarded as middle Holocene, between ~5 and 3 kyr.

4.1.5. Qft4

Qft4 deposits occur along the entire Red Rock piedmont, but are restricted in aerial extent relative to the larger Qft2/3 and Qft4a deposits. North of Big Sheep Creek Qft4 deposits are confined to channels inset into the older fan units. In the south, Qft4 deposits bury Qft4a fans in the Red Rock hanging wall and are inset into Qft4a treads in the adjacent footwall (Fig. 4). Qft4 terraces along Big Sheep Creek are low, gravel capped surfaces 0–3 m above the modern river that are entrenched within older surfaces. Qft4 deposits exhibit a pronounced bar and swale morphology as well as modern, active channel beds. Qft4 deposits are similar in clast composition to the older fan units but are typically finer grained, dominated by sand and silt. There is little to no pedogenic carbonate in Qft4 deposits. A radiocarbon age of 1.3 kyr from 0.75 m depth indicates a late Holocene age of this unit (Table 2, Fig. 3).

4.2. Fault segmentation

4.2.1. Fan unit distribution

From Little Sheep Creek to Garr Canyon (km 0–8 on Fig. 3), exposures of Qft4 and Qft4a surfaces dominate. Here, they overlap rather than entrench older deposits. To the north, from Garr Canyon to Dry Canyon (Fig. 3, km 9–17), Qft4a and Qft4 units cover reduced landscape and are progressively more entrenched into the Qft2/3 deposits. North of Dry Canyon (Fig. 3, km 17–27) the hanging wall is dominated by Qft2/3 exposures and isolated exposures of Qft1. Here, both Qft4a and Qft4 deposits are deeply entrenched to a depth of 3–10 m within the older fan units.

4.2.2. Scarp distribution

Prominent scarps along the range front offset Qf4a surfaces nearly continuously from just south of Little Sheep Creek to ~0.5 km north of Chute Canyon (Fig. 3, km 0–7), where buried by a landslide. Scarps heights between Little Sheep Creek and Chute Canyon vary from ~1 m to more than 10 m in the central portion of this fault segment; however, Qft4 surfaces are not faulted along this strike length. At Garr Canyon, the range front steps ~0.5 km eastward and no scarps are present within any fan unit. Scarps appear again ~0.5 km north of Garr Canyon. Less prominent scarps then extend discontinuously north until ~1 km north of Little Water Canyon (Fig. 3, km 9–19). Qft3 deposits at the mouths of Big Sheep Creek, Dry Canyon, and several other unnamed drainages are offset, but Qft4 and Qft4a surfaces are not. From south of McKnight Canyon to where the fault dies out north of Limekiln Creek (Fig. 3, km 20–27), the range front steps ~0.5 km eastward. Along the northern fault trace, one Qft1 deposit preserves evidence of rupture; however, fault scarps were not observed in younger surfaces (Fig. 3).

4.2.3. Footwall geomorphic indices

From Little Sheep Creek to Garr Canyon (Fig. 3, km 0–8) footwall drainage basin channel long profiles abruptly steepen downstream towards the range front (Fig. 4). The convexities in the long profiles are evident in the length–gradient (*SL*) indices for these channels (Fig. 5). *SL* values are high, indicating steeper relative slopes, near stream mouths at 400–600 m and decrease up stream to 200–300 m in many of the southern drainages. The upper channel values are equivalent to those observed in the control basins and characterize channel slopes within Beaverhead Group. Long profiles from Garr Canyon to Big Sheep Creek (Fig. 3, km 8–12) are not distinctive from those observed farther north. *SL* values are consistently low from Garr Canyon to Big Sheep Creek (150–300 m) and consistently high north of Big Sheep Creek to the northern extreme of the Red Rock fault (300–600 m). Although high, the *SL* values north of Big Sheep Creek do not increase towards the range front.

Hypsometric integrals collected from drainages south of Garr Canyon are large relative to the rest of the data, indicating greater basin areas at high elevations. Hypsometric integrals display a subtle trend of decreasing values to the north (Fig. 6), where more of the basin area is closer to base level. Kelmbeck Creek and Limekiln Creek basins, at the northern end of the fault (Fig. 3, km 24–25), exhibit anomalously large integral values relative to overall trends.

V/A ratio values for basins south of Garr Canyon are distinctive from others along strike. A Mann–Whitney test of significance showed that southern basins are distinguished (at $\alpha = 0.05$) by high *V/A* values, whereas basins north of Garr Canyon are indistinguishable from control basins with lower *V/A* values. Higher *V/A* values reflect deeper, more incised basins. In contrast to the other morphometric indices, area/elongation values and basin asymmetries show no pattern to variance along strike.

4.3. Manifestation of fault activity along Big Sheep Creek

In addition to the prominent scarps and knick point at the mouth of Big Sheep Creek, a number of fault related morphologic trends are observed upstream of the fault. For ~200 m upstream from the knick point, Qft4a and Qft4

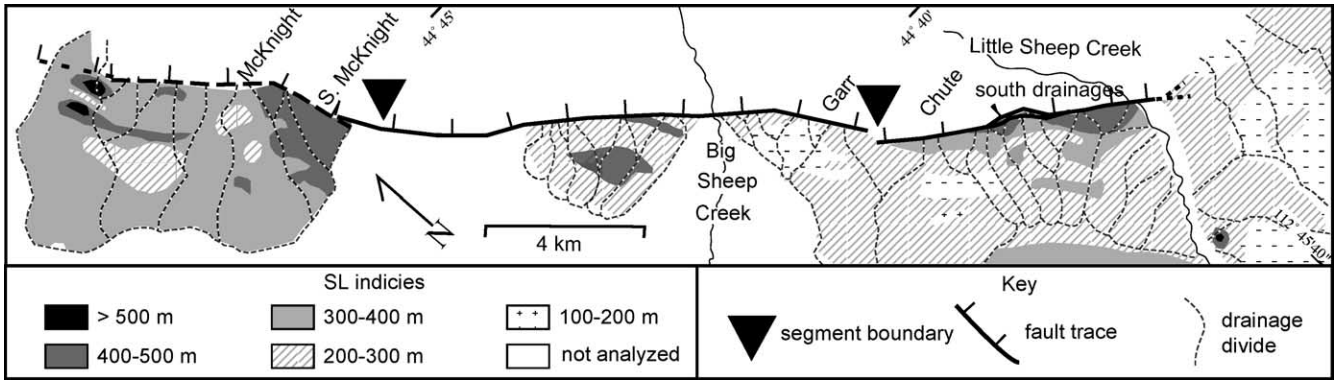

Fig. 5. Contour map of stream length (*SL*) values computed for all analyzed channels. Major drainages are named and basins are outlined by their divides. Increased *SL* values proximal to the range front imply channel steepening in response to fault motion. In the south, persistent values of 100–300 m deviate to higher values proximal to the range front. Segment breaks inferred from this study are shown for reference.

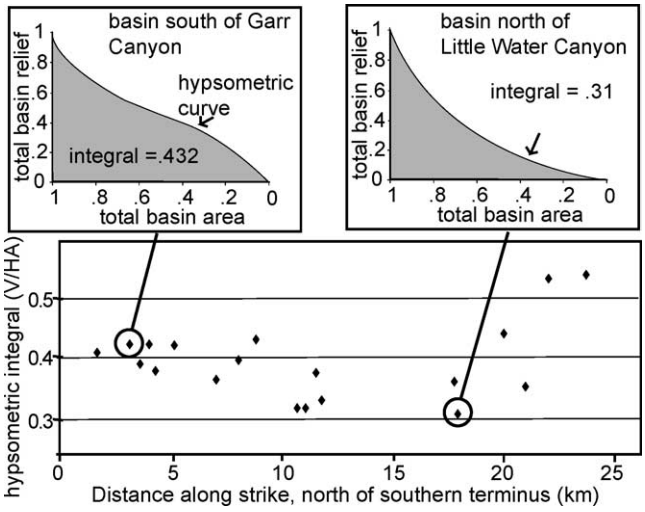

Fig. 6. Footwall drainage basin hypsometric integral values versus position relative to the southern fault termination. Two examples of hypsometric curves are shown for reference.

surfaces are difficult to distinguish within a complex suite of small, discontinuous terrace surfaces nested within a broad Qft3 surface (Fig. 7). The discontinuous terraces are interpreted to record previous rupture and knick point generation and are not observed elsewhere upstream. Qft1, Qft2, and Qft3 surfaces converge upstream for ~6 km, from the fault to where the river flows over the resistant quartzite of the Pennsylvanian Quadrant Formation. No terraces are preserved along the Quadrant channel reach. Upstream of the Quadrant, a complete suite of diverging terrace surfaces is preserved. The Big Sheep Creek channel long profile also varies upstream and downstream of the Quadrant outcrop belt. Upstream, the channel exhibits an overall concave-up profile. Within the Quadrant Formation, the river has a low gradient and high sinuosity. Downstream, the channel gradient steepens toward the fault, resulting in a convex-up profile. Terrace convergence towards the Quadrant channel reach implies that slow river incision into the quartzite sets a local base level for Big Sheep Creek

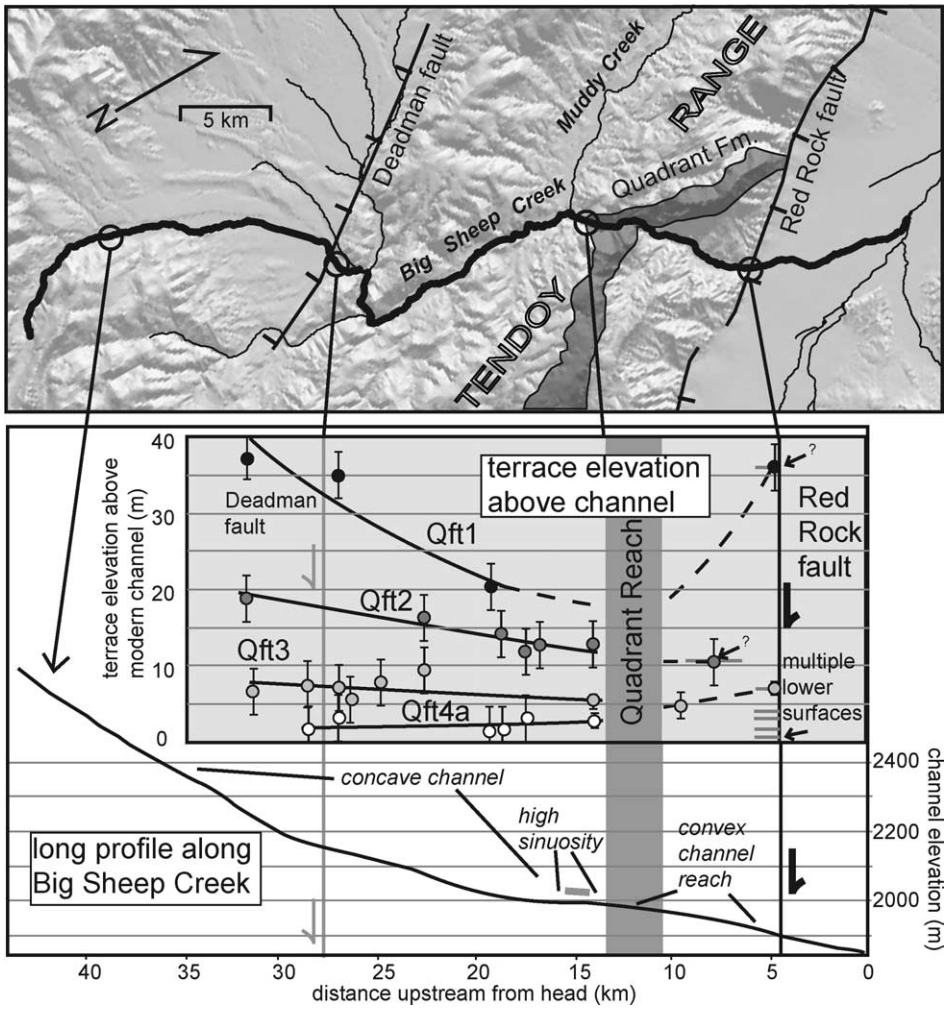

Fig. 7. Terrace and channel profiles along Big Sheep Creek plotted upstream from the Red Rock River. The inset graph displays surveyed heights of Qft1 through Qft4a terrace surfaces above the modern channel. Best fit trend lines are dashed where inferred. The larger graph displays the Big Sheep Creek long profile adjacent to the surveyed terraces.

upstream and pins the channel elevation between the fault and the Quadrant outcrop belt.

5. Discussion

5.1. Segmentation along the Red Rock fault

Fault segments resolved from surface rupture utilize a direct link between geomorphic features and recent fault motion. Surface ruptures from the three most recent events along the Red Rock fault delineate three segments (Figs. 2 and 3). As shown by the trenching study (Stickney and Bartholomew, 1987), our data confirm that the southern segment last ruptured ~3 kyr. Strong evidence for the 3 kyr event defines the southern segment, which extends ~8 km from Little Sheep Creek to Garr Canyon (Fig. 3, km 0–8). The central segment extends from Garr Canyon to ~1 km north of Little Water Canyon and is identified by a definitive last rupture age of 10–3 kyr (Fig. 3, km 8–19). This event or events also ruptured part of the southern segment, as indicated by multiple southern fault scarps and by the 9 kyr minimum rupture age derived from the Little Sheep Creek trench (Stickney and Bartholomew, 1987). Although not directly dated, the Big Sheep Creek channel is inset into a surface offset by the 10–3 kyr event upstream of the ~2 m knick zone. This implies that the knick zone is the result of at least one additional, more recent rupture event. While no definitive evidence remains, the southern terminus of the central segment likely experienced surface rupture during the 3 kyr event. The lack of offset in the Qft4a surface at Dry Canyon indicates that the 3 kyr rupture does not extend across the entire central segment but, rather, it is confined between Garr Canyon and Dry Canyon. The northern segment, extending from ~1 km north of Little Water Canyon until the fault is lost in the bedrock just north of Limekiln Canyon (Fig. 3, km 19–27), is characterized by a lack of recent rupture, with the last event occurring at 10–15 kyr. These surface rupture patterns define the southern (Fig. 3, km 0–8), central (km 9–19), and northern (km 19–27) segments of the Red Rock fault. The three-segment framework generates testable hypotheses that can be compared with fault segmentation defined by other criteria.

At least two surface rupturing events within the last 10 kyr (>4 m of offset in a 4.5 kyr surface at Chute Canyon) define the southern segment. Here, the rapid down dropping of Red Rock Valley controls channel metrics and fan geometries proximal to the fault trace. This has served to both create accommodation space for the steep, vertically aggrading footwall fans along this segment and to produce the base level fall which generates the deeply entrenched, steep footwall channels proximal to the range front. The southern segment has distinctive channel convexities and high *SL* values proximal to the fault trace (Fig. 5).

The central segment has experienced less tectonic activity than the south in the last 10 kyr based on lower *V/A* ratios and an absence of channel response to faulting. *SL* values are higher from watersheds with more resistant bedrock of the Tendoy thrust sheet, north of Big Sheep Creek; however, the *SL* values show no perturbation proximal to the fault. The lack of scarps at Garr Canyon accompanied by a lateral step in the mountain front strengthens the interpretation of a segment boundary at this location. A break in surface rupture accompanying a lateral step in an active range front is a trait commonly used to define normal fault segment boundaries (Crone and Haller, 1991; Zhang et al., 1991).

We define the boundary between the central and northern segments by the loss of fault scarps north of Little Water Canyon, near the segment boundary reported in Haller (1988). Basin metrics, despite failure to distinguish this segment boundary, agree with other data indicating an absence of recent tectonism along the northern segment. The high *SL* values observed within the northern segment result from Paleozoic bedrock in the hanging wall of the Tendoy thrust sheet thrusted atop the Beaverhead Formation. The two anomalously high hypsometric values from the northern end of the fault have similar lithologic control (Fig. 2). The lack of northern segment catchments with *SL* gradients that steepen toward the Red Rock fault implies a persistent lack of surface rupture. The fault trace disappears in Paleozoic bedrock at the northern mapped limit of this segment. Nearby, the hanging wall fan deposits incompletely bury isolated outcrops of Tertiary aged bedrock. Tertiary outcrops are not observed elsewhere in the Red Rock hanging wall, implying that total displacement is least in the northern segment.

5.2. Response characteristics of tectonic geomorphic indices

The suite of fault plane, hanging wall, and footwall data sets constrain the kinematic history of the Red Rock fault and more generally the response dynamics of drainage basins and fan systems to nascent extension. Surface rupture patterns, scarp morphology, fan deposition, channel gradients, and basin *V/A* ratios indicate an increase in tectonism southward, especially in the southern segment.

Footwall indices that are sensitive to the three-dimensional geometry of a basin (e.g. long profiles, *SL* gradients) integrate tectonic events over 10^4–10^5 yrs, fluvial systems respond to a base level drop first through incision. This is apparent in channel profiles proximal to the southern range front. *V/A* ratios and hypsometric values show this relationship in a more subtle fashion because these indices integrate topography over an entire basin. Comparatively, basin area metrics like elongation and asymmetry, which respond over longer times, do not record the along strike gradient in Red Rock fault activity. The processes that effect basin area distribution, such as drainage capture and lateral channel erosion, operate over longer time intervals than

channel incision. The Red Rock fault has likely not been active long enough for basin area metrics to respond.

The majority of the footwall relief along the Tendoy mountain front was inherited from the Sevier thrust front rather than as a direct manifestation of Red rock displacement. The greatest relief along the central and northern segments is coincident with a structural culmination in the Tendoy thrust sheet. The proximal footwall of the southern segment is underlain by Beaverhead Group and exhibits lower total relief.

Along Big Sheep Creek, eastward divergence of terraces downstream from the Quadrant Formation results from channels responding to the base level fall generated at the fault. Each offset produces channel oversteepening (knick zone), which migrates upstream eroding alluvial surfaces. The resistant Quadrant Formation supports a local base level, which inhibits upstream knick zone migration and isolates the upstream reach of Big Sheep Creek from the effects of Red Rock faulting.

Utilizing the ages of fan surfaces, estimates of the relative response times and sensitivities of the various geomorphic indices can be made (Fig. 8). Surface ruptures record individual offset events, although the ephemeral nature of fault scarps and overprinting by subsequent tectonism limits the longevity of these features. Comparatively, fan distribution and fan metrics operate and preserve integrated records of multiple tectonic events over $\sim 10^3$–10^4 yrs. Three-dimensional channel metrics respond at roughly the same time scales as fans, but may require a greater amount of total fault offset (and thus time) to develop a detectable tectonic signature. Basin area indices respond slower still, integrating tectonics over 10^{6+} yrs.

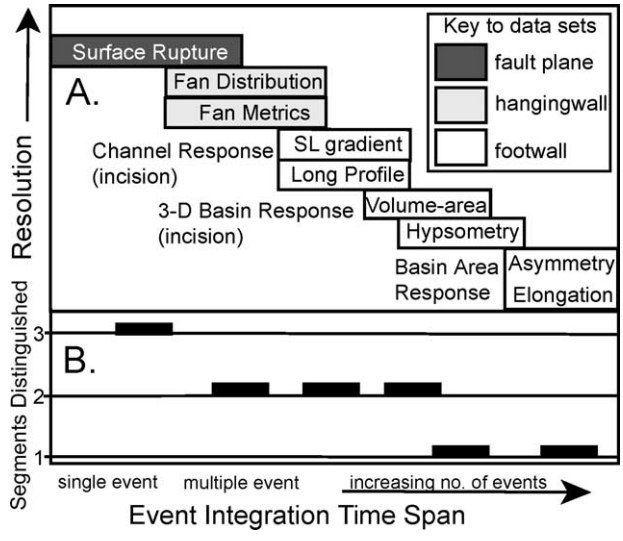

Fig. 8. (A) Relative sensitivity (ability to record individual or small events) of various geomorphic data to isolate fault rupture. The indices are shaded to indicate whether the data sets sample the fault plane, hanging wall, or footwall. (B) Indicates the number of segments distinguished along the Red Rock fault by each data set, as a proxy for the resolution capabilities of each index.

5.3. Red Rock fault kinematics and dynamics

Records of tectonism, which integrate multiple events, such as three-dimensional basin metrics, broadly agree with single event records in elucidating the displacement gradient along the Red Rock fault. Densmore et al. (2004) interpreted the lack of scarps along the northern segment as evidence of recent northward fault propagation. Alternatively, the lack of northern fault scarps may be an indication of persistently slow slip rates. The west dipping Monument Hill fault system, along eastern Red Rock Valley also has evidence for multiple recent ruptures, with at least one likely in the Holocene. Displacement transfer between the northern Red Rock fault and southern Monument Hill fault may occur during Red Rock Valley earthquakes. It is worth noting that the 1999 5.3 m_b 'Kidd' earthquake did not rupture the ground surface.

Stickney et al. (2000), suggests slip rates of 0.2–1.0 mm/yr for the southern Red Rock fault and <0.2 mm/yr for the north. Based on the height of scarps produced during the 3 kyr rupture, the southern segment has experienced a maximum slip rate of 1.33 and 2.0 mm/yr at Little Sheep Creek and Chute Canyon, respectively (Fig. 9). The rates are likely higher in the middle of the southern segment, where the scarps are highest. The rates should be regarded as maximums as they are based on elapsed time since the most recent rupture. In the central segment, maximum slip rates based on an older, early Holocene (9–10 kyr) event are 0.6 and 0.9 mm/yr at Big Sheep Creek and Dry Canyon, respectively. At Big Sheep Creek, the measured scarp height in the Qft3 surface is likely the result of displacement from both the middle (3 kyr) and early Holocene (9–10 kyr) events. Interpreting the 6 m scarp at Big Sheep Creek as a 4 m offset at 10 kyr and a 2 m (knick zone height) offset at 3 kyr, yields slip rates of 0.57 mm/yr and 0.67 mm/yr, respectively. Since the rate determined since the 3 kyr rupture is expected to be a maximum, the slower slip rate based on the early Holocene offset is likely more characteristic at this location.

A 'bell' shape displacement pattern is defined by early Holocene scarp heights in the central segment. The scarp heights observed in the southern segment display a similar pattern, with the greatest displacement in the middle of the segment. This pattern is consistent with the fault segments slipping independently. Slip in the central segment associated with ~ 3 kyr rupture is an indication of strain communication between the two segments and suggests fault linked in the subsurface, similar to the 1911 Pleasant Valley, NV and 1983 Borah Peak, ID events. Given the likely youthfulness of the Red Rock fault, this pattern of intermittent coalescence may be an early developmental stage of normal faulting. The behavior is consistent with normal fault zone evolutionary models where multiple independent surfaces nucleate and slip, coalescing into a more continuous fault zone over time (Peacock and Sanders 1991; Anders and Schlische 1994; Dawers and Anders 1995).

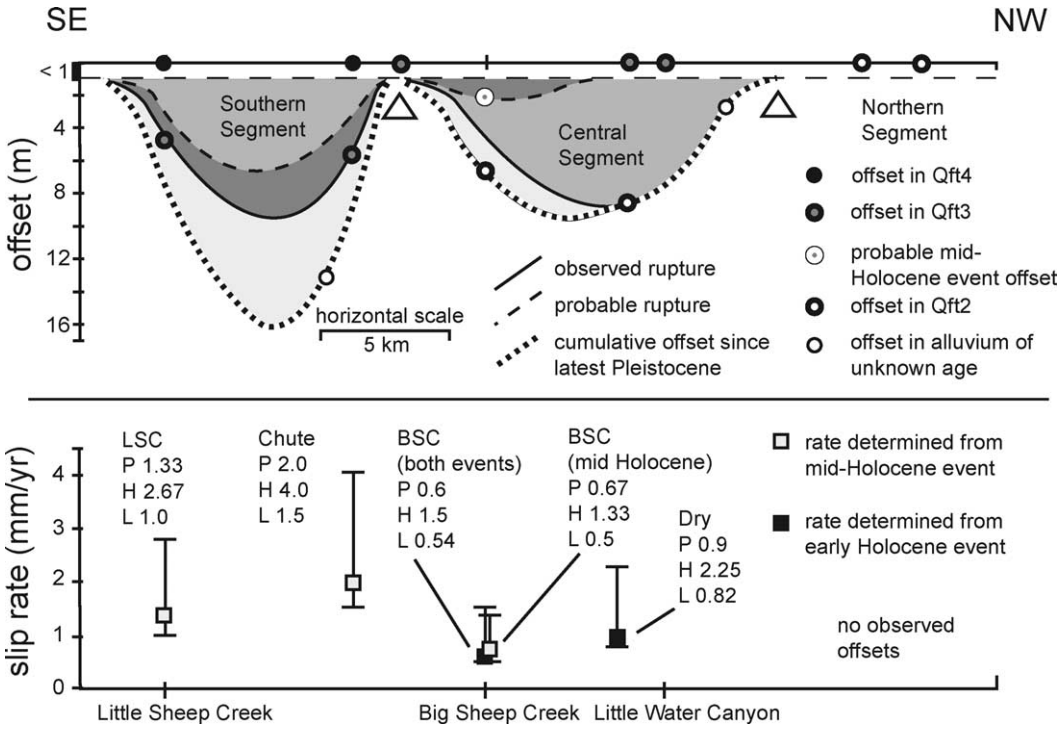

Fig. 9. Rupture patterns and slip rates determined from offset fan and terrace surfaces along the Red Rock fault, plotted along strike. In the top plot; filled circles represent observed offset magnitudes in alluvium of various ages. A mid-Holocene offset was inferred from the 2 m high knick point in Big Sheep Creek, just upstream of the scarp. The filled curves, dark shading for the mid-Holocene event and lighter shading for the early Holocene event, represent individual rupture extents. The curve shapes are constrained by observed cumulative offsets. Segment boundaries are delineated by triangles. In the bottom plot, slip rates were determined from measured offsets and rupture ages at Little Sheep Creek (LSC), Chute Canyon, Big Sheep Creek (BSC), and Dry Canyon. Probable rates (*P*) were determined from likely event ages. High (H) and low (L) bounding rates were determined from the ages of offset alluvium. Excepting BSC, rates were determined from the most recent offset at each site and should be regarded as maximums. Note the agreement in rates determined at BSC from both the mid-Holocene event and the cumulative offset over both events.

5.4. Tectonic significance

Geologic constraints and displacement–length relationships suggest throw on the Red Rock fault is <1 km. Slip rates near 1 mm/yr support a 1 Myr old Red Rock fault. A youthful Red Rock fault is consistent with the eastward decrease in the age of faulting along the Yellowstone hot spot track (Stickney and Bartholomew, 1987; Crone and Haller, 1991; Pierce and Morgan, 1992; Fritz and Sears, 1993; Densmore et al., 2004). The Red Rock fault stands in contrast to the much larger and older Lost River, Lemhi, and Beaverhead faults to the west (Fig. 1, inset).

6. Conclusions

The Red Rock fault exhibits variable displacement along strike since at least the Late Pleistocene. Based on the distribution of dated rupture events, three segments are resolvable along the fault, with a segment break similar to that previously suggested near Little Water Canyon, and a previously unidentified break at Garr Canyon. Multiple Holocene rupturing events are evidence of rapid, ongoing fault slip along the southern segment. The central and northern segments exhibit progressively lesser amounts of recent offset. The northern segment has not experienced significant surface rupture since at least the Late Pleistocene and total displacement along the fault in the north is small.

Topographic and geologic features commonly used to delineate fault segmentation record displacement over diverse temporal and spatial scales. The relative sensitivity of these features is determined from the segmentation records preserved by relative and absolute dating of landforms. The concordance of segmentation records preserved in alluvial fans and channel profiles imply that fluvial systems have the ability to respond rapidly (10^3–10^5 yrs) to a base level fall resulting from a fault offset. Initially this occurs through channel incision and followed later by slower processes that affect planimetric basin metrics such as stream capture.

The record of fault offset preserved in the drainage basin metrics indicates that the distribution of Holocene and Late Pleistocene activity recorded by Red Rock surface ruptures reflects the lifespan of the fault as well. Given the limited spatial extent of a tectonic signal in the Big Sheep Creek channel and the discordance between the locations of the highest range front topography and the areas of most rapid fault slip, the footwall topography must retain a significant

degree of inherited morphology. This implies that the Red Rock fault has not been active long enough to impact all aspects of footwall topography.

Assigning likely rupture ages to fault scarps yields maximum slip rates of 1.33–2.0 mm/yr for the southern segment and 0.6–0.9 mm/yr for the central segment. The interpreted distribution of offset associated with recent ruptures suggests that segments mainly behave independently, but maybe in the process of coalescing in the shallow crust. Finally, the apparent youth of the Red Rock fault, when compared with more westward faults within the Centennial Tectonic Belt, strengthens interpretations of an eastward progression of fault initiation in response to Yellowstone hot spot migration.

Acknowledgements

This research was supported by DOI-USGS-EDMAP grant 01HQA0188 awarded to Anastasio, a grant from the American Association of Petroleum Geologists Grants in Aid program awarded to Harkins, and DOI-USGS-EDMAP grant 02HQAG0081 awarded to Anastasio, Harkins, and Pazzaglia. The authors gratefully acknowledge the field assistance of Diana Latta and Michael Newton and the hospitality of Arlene Greensladd over two field seasons. The research benefited from discussions with Jerry Bartholomew, Michael Stickney, Kathy Haller, and Edward Evenson. Nancye Dawers and an anonymous reviewer for JSG are thanked for their suggestions to improve the manuscript.

References

Anders, M.H., 1997. The Yellowstone–Snake River Plain migrating deformation field; causes and implications for assessing North American Plate velocity. The Geological Society of America 1997 Annual Meeting, Abstracts with Programs, A-166.

Anders, M.H., Schlische, R.W., 1994. Overlapping faults, intrabasin highs, and the growth of normal faults. Journal of Geology 102, 165–180.

Anders, M.H., Geissman, J.W., Piety, L.A., Sullivan, J.T., 1989. Parabolic distribution of circum-eastern Snake River Plain seismicity and latest Quaternary faulting; migratory pattern and association with the Yellowstone hot spot. Journal of Geophysical Research 95, 1589–1621.

Birkeland, P.W., 1999. Soils and Geomorphology. Oxford University Press, New York.

Bull, W.B., 1961. Tectonic significance of radial profiles of alluvial fans in western Fresno County, California. Article 75: US Geological Society Professional Paper, pp. B182–B184.

Bull, W.B., McFadden, L.D., 1977. Tectonic geomorphology north and south of the Garlock fault, California. In: Doerhing, D.O. (Ed.), Geomorphology of Arid Regions Proceedings of the Eighth Annual Geomorphology Symposium. State University of New York at Binghamton, pp. 115–138.

Cowie, P.A., 1998. A healing–reloading feedback control on the growth rate of seismogenic faults. Journal of Structural Geology 20, 1075–1087.

Cox, R.T., 1994. Analysis of drainage basin symmetry as a rapid technique to identify areas of possible Quaternary tilt-block tectonics; an example from the Mississippi Embayment. Geological Society of America Bulletin 106, 571–581.

Crone, A.J., Haller, K.M., 1991. Segmentation and the coseismic behavior of Basin and Range normal faults: examples from east-central Idaho and southwestern Montana, USA. Journal of Structural Geology 13, 151–164.

Dawers, N.H., Anders, M.H., 1995. Displacement–length scaling and fault linkage. Journal of Structural Geology 17, 607–614.

Denny, C.S., 1967. Fans and pediments. American Journal of Science 265, 81–105.

Densmore, A.L., Dawers, N.H., Gupta, S., Guidon, R., Goldin, T., 2004. Footwall topographic development during continental extension. Journal of Geophysical Research 109. 16pp.

DePolo, C.M., Clack, D.G., Slemmons, B., Ramelli, A.R., 1991. Historical surface faulting in the Basin and Range province, western North America: implications for fault segmentation. Journal of Structural Geology 13, 123–136.

Dodge, R.L., Grose, L.T., 1980. Tectonic and geomorphic evolution of the Black Rock Fault, northwestern Nevada. Proceedings of conference X; earthquake hazards along the Wasatch and Sierra Nevada frontal fault zones. US Geological Survey Open-File Report 80-801, pp. 494–508.

Fields, R.W., Rasmussen, D.L., Tabrum, A.R., Nichols, R., 1985. Cenozoic rocks of the intermontane basins of western Montana and eastern Idaho; a summary. In: Flores, R.M., Kaplan, S.S. (Eds.), Cenozoic Paleogeography of the West Central United States Rocky Mountain Section. Society of Economic Paleontologists and Mineralogists, Paleogeography Symposium 3, pp. 9–36.

Frankel, K.L., 2002. Quantitative topographic differences between erosionally exhumed and tectonically active mountain fronts: implications for Late-Cenozoic evolution of the southern Rocky Mountains. MS Thesis, Lehigh University.

Franklin, S.E., 1987. Geomorphometric processing of digital elevation models. Computers and Geosciences 13, 603–609.

Fritz, W.J., Sears, J.W., 1993. Tectonics of the Yellowstone hotspot wake in southwestern Montana. Geology 21, 427–430.

Gile, L.H., Peterson, F.F., Grossman, R.B., 1966. Morphological and genetic sequences of carbonate accumulation in desert soils. Soil Science 101, 347–360.

Greenwell, R.A., 1997. Alluvial fan development, the key to segmentation of the Red Rock fault, Southwestern Montana. MS Thesis, University of South Carolina.

Hack, J.T., 1973. Stream-profile analysis and stream-gradient index. US Geological Survey Journal of Research 1, 421–429.

Haller, K.M., 1988. Proposed segmentation of the Lemhi and Beaverhead faults, Idaho, and Red Rock fault, Montana—evidence from studies of fault scarp morphology. Geological Society of America Abstracts with Programs 20, 418–419.

Hare, P.W., Gardner, T.W., 1985. Geomorphic indicators of vertical neotectonism along convergent plate margins, Nicoya Peninsula, Costa Rica. Tectonic Geomorphology, Binghamton Symposia in Geomorphology: International Series 15, 75–104.

Harkins, N.W., Latta, D.K., Anastasio, D.J., Pazzaglia, F.J., 2002. Surficial and bedrock map of the Dixon Mountain 7.5′ quadrangle, SW Montana. Montana Bureau of Mines and Geology Open File Report 495, scale 1: 24,000.

Harkins, N.W., Newton, M., Pazzaglia, F.J., Anastasio, D.J., 2003. Surficial and bedrock map of the Caboose Canyon 7.5′ quadrangle, SW Montana. Montana Bureau of Mines and Geology Open File Report 494, scale 1:24,000.

Johnson, P.P., 1981. Geology along the Red Rock fault and adjacent Red Rock Basin, Beaverhead County, Montana. Montana Geological Society 1981 Field Conference, SW Montana, pp. 245–251.

Klecker, R.A., 1980. Paleozoic sedimentology of the Dixon Mountain–Little Water Canyon Area, Beaverhead County, Montana. MS Thesis, Oregon State University.

Lonn, J.D., Skipp, B., Ruppel, E.T., Janecke, S.U., Perry, W.J., Sears, J.W.,

Bartholomew, M.J., Stickney, M.C., Fritz, W.J., Hurlow, H.A., Thomas, R.C., 2000. Geologic map of the Lima 30′×60′ Quadrangle, Southwest Montana. Montana Bureau of Mines and Geology Open File 408, scale 1:100,000.

Lustig, L.K., 1965. Clastic sedimentation in Deep Springs Valley, California. US Geological Survey Professional Paper 352-F.

McCalpin, J.P., 1996. Paleoseismology in extensional tectonic environments. Paleoseismology, International Geophysics Series 62, 85–146.

McDowell, R.J., 1989. Effects of syn-sedimentary basement tectonics on fold thrust geometry, Southwestern Montana. PhD Thesis, University of Kentucky, Lexington.

Peacock, D.C.P., Sanderson, D.J., 1991. Displacements, segment linkage and relay ramps in normal fault zones. Journal of Structural Geology 13, 721–733.

Pierce, K.L., Morgan, L.A., 1992. The track of the Yellowstone hot spot: volcanism, faulting, and uplift. In: Link, P.K., Kuntz, M.A., Platt, L.B. (Eds.), Regional Geology of Eastern Idaho and Western Wyoming. Geological Society of America Memoir 179, pp. 1–51.

Pike, R.J., Wilson, S.E., 1971. Elevation-relief ratio, hypsometric integral, and geomorphic area-altitude analysis. Geological Society of America Bulletin 82, 1079–1084.

Reheis, M.C., 1987. Soils in granitic alluvium in humid and semi-arid climates along Rock Creek, Carbon County, Montana. US Geological Survey Bulletin 1590-D, 41pp.

Ritter, J.B., Miller, J.R., Enzel, Y., Howes, S.D., Nadon, G., Grubb, M.D., Hoover, K.A., Olsen, T., Reneau, S.L., Sack, D., Summa, C.L., Taylor, I., Touysinhthiphonexay, K.C.N., Yodis, E.G., Schneider, N.P., Ritter, D.F., Wells, S.G., 1993. Quaternary evolution of the Cedar Creek Alluvial Fan, Montana. Geomorphology 8, 287–304.

Scholten, R.K., Keenmon, K.A., Kupsch, W.O., 1955. Geology of the Lima region, Southwestern Montana and adjacent Idaho. Geological Society of America Bulletin 66, 345–404.

Schwartz, D.P., Swan III., F.H., Hanson, K.L., 1982. Fault zone segmentation based on geometry and recurrence; the Wasatch fault zone, Utah. Seismological Society of America, Abstracts, Earthquake Notes 54, 60.

Stickney, M.C., Bartholomew, M.J., 1987. Seismicity and late Quaternary faulting of the Northern Basin and Range province, Montana and Idaho. Bulletin of the Seismological Society of America 77, 1602–1625.

Stickney, M.C., Lageson, D.R., 2002. Seismotectonics of the 20 August 1999 Red Rock Valley, Montana, Earthquake. Bulletin of the Seismological Society of America 92, 2449–2464.

Stickney, M.C., Bartholomew, M.J., Wilde, E.M., 1987. Trench logs across the Red Rock, Blacktail, Lima Reservoir, Georgia Gulch, Vendome and Divide faults, Montana. Geological Society of America, Rocky Mtn. Section. 40th Annual Meeting Abstracts with Programs 19, 336–337.

Stickney, M.C., Haller, K.M., Machette, M.N., 2000. Quaternary faults and seismicity in western Montana. 1:750,000 scale map with text. MBMG Special Publication No. 114.

Strahler, A.N., 1952. Hypsometric (area-altitude) analysis of erosional topography. Geological Society of America Bulletin 63, 1117–1142.

Turko, J.M., Knuepfer, P.L.K., 1991. Late Quaternary fault segmentation from analysis of scarp morphology. Geology 19, 718–721.

Wheeler, R.L., 1987. Boundaries between segments of normal faults; criteria for recognition and interpretation. In: Proceedings of Conference XXXIX; Directions in Paleoseismology. Open file report, US Geological Survey, pp. 385–398.

Williams, N.S., 1984. Stratigraphy and structure of the east-central Tendoy Range, Southwestern Montana. MS Thesis, University of North Carolina, Chapel Hill.

Zhang, P., Slemmons, D.B., Mao, F., 1991. Geometric pattern, rupture termination and fault segmentation of the Dixie Valley–Pleasant Valley active normal fault system, Nevada, USA. Journal of Structural Geology 13, 165–176.